DOI 10.1007/s10812-018-0631-7
Journal of Applied Spectroscopy, Vol. 85, No. 1, March, 2018 (Russian Original Vol. 85, No. 1, January–February, 2018)

QUANTITATIVE ANALYSIS OF Ca, Mg, AND K IN THE ROOTS OF *Angelica pubescens f. biserrata* BY LASER-INDUCED BREAKDOWN SPECTROSCOPY COMBINED WITH ARTIFICIAL NEURAL NETWORKS

J. Wang,[a] M. Shi,[a] P. Zheng,[a*] Sh. Xue,[a] and R. Peng[b]

UDC 543.42

Laser-induced breakdown spectroscopy has been applied for the quantitative analysis of Ca, Mg, and K in the roots of Angelica pubescens Maxim. f. biserrata Shan et Yuan used in traditional Chinese medicine. Ca II 317.993 nm, Mg I 517.268 nm, and K I 769.896 nm spectral lines have been chosen to set up calibration models for the analysis using the external standard and artificial neural network methods. The linear correlation coefficients of the predicted concentrations versus the standard concentrations of six samples determined by the artificial neural network method are 0.9896, 0.9945, and 0.9911 for Ca, Mg, and K, respectively, which are better than for the external standard method. The artificial neural network method also gives better performance comparing with the external standard method for the average and maximum relative errors, average relative standard deviations, and most maximum relative standard deviations of the predicted concentrations of Ca, Mg, and K in the six samples. Finally, it is proved that the artificial neural network method gives better performance compared to the external standard method for the quantitative analysis of Ca, Mg, and K in the roots of Angelica pubescens.

Keywords: *laser-induced breakdown spectroscopy, roots of Angelica pubescens, artificial neural networks, quantitative analysis.*

Introduction. The roots of *Angelica pubescens Maxim. f. biserrata Shan et Yuan* are related to one of the most popular traditional Chinese medicines. They have efficient antiphlogistic, anesthetic, and antitumor properties [1]. Osthole in the roots of *Angelica pubescens* can antagonize Ca^{2+}, prevent extracellular from calcium ions flowing into cells, reduce the force of myocardial contraction and the oxygen consumption of myocardium, and decrease the blood pressure. In the functional process of traditional Chinese medicine, the synergy of metal elements cannot be ignored. Neuromuscular excitation is related to the concentration of Mg and Ca in the blood. The antiphlogistic and anticancer Chinese medicines always contain abundant Ca and K, while the antidotal Chinese medicines contain abundant Ca and Mg. Appropriate concentrations of metal elements not only assist human growth but also can enhance immunity.

High-performance laboratory techniques, such as inductively coupled plasma-optical emission spectroscopy (ICP-OES) [2], atomic absorption spectrometry (AAS) [3] and inductively coupled plasma mass spectrometry (ICP-MS) [4] have been used to detect the metal elements in traditional Chinese medicine. However, these techniques consume large amounts of energy and are operated at high temperatures or under vacuum, and also require complex sample preparation, so are impractical for portable measurements. Moreover, their operating costs are high and are therefore unsuitable for continuous monitoring.

Laser-induced breakdown spectroscopy (LIBS) is a technique in which laser pulses are used to ablate a target, and emission spectra of the resulting plasma are collected and analyzed. Over the last few decades, the feasibility of LIBS as an analytical technique has been demonstrated by a number of applications on solids [5–9], liquids [10–14], gases [15–17], or aerosol [18–20] samples because of the technique advantages for *in situ* and real-time analysis without or with little need for sample preparation. It is worth mentioning that the main problems related to the LIBS analysis are limited sensitivity and

*To whom correspondence should be addressed.

[a]Chongqing Municipal Level Key Laboratory of Photoelectronic Information Sensing and Transmitting Technology, College of Optoelectronic Engineering, Chongqing University of Posts; and Telecommunications; Chongqing 400065, China; email: zhengpc@cqupt.edu.cn; [b]Chongqing Academy of Chinese Medicine, Chongqing 400065, China. Abstract of article is published in Zhurnal Prikladnoi Spektroskopii, Vol. 85, No. 1, p. 175, January–February, 2018.

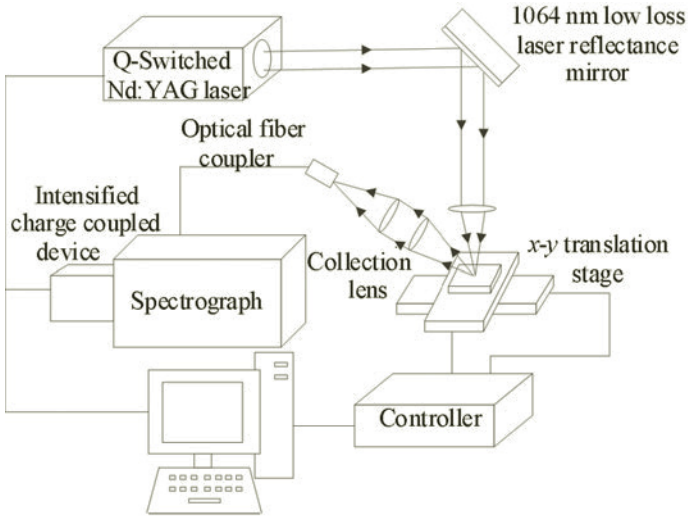

Fig. 1. Schematic diagram of the laser-induced breakdown spectroscopy experimental setup.

the poor precision of the technique, which also affect the global accuracy of the results. Therefore, LIBS data interpretation, including retrieving quantitative information from the measured spectra, is still a subject for research and development and is especially important when the target properties and composition are *a priori* unknown. The artificial neural network (ANN) method is a multiple nonlinear calibration model that can calibrate complex nonlinear relationships in complex matrices [21–25]. Therefore, the ANN method can be introduced to eliminate some interference during the process of quantitative analysis of the LIBS technique.

In the present work, the LIBS technology combined with artificial neural network (ANN) method was employed to quantitatively analyze the concentrations of Ca, Mg, and K in the roots of *Angelica pubescens* compared with the external standard method.

Experimental. A schematic view of the experimental setup is presented in Fig. 1. A Q-switched Nd:YAG laser (Big Sky Laser Technology, Ultra 100), at the fundamental wavelength of 1064 nm with a pulse duration of 5.82 ns, maximum repetition rate of 20 Hz, and maximum pulse energy of 100 mJ, is used as the excitation laser. The laser energy can be switched by changing the Q delay time, which can be measured by a laser power meter. The laser beam is focused perpendicular to the sample surface on a two-dimensional translation stage, which is controlled by a controller (Zolix SC300-2A) with a plano-convex lens (f = 100 mm) to produce intense and transient plasma. The light emitted from the plasma is focused by a microscope objective lenses system and collected by a 2-m long multimode silica fiber. The light is then transmitted through the fiber to the entrance of a computerized Czerny–Turner spectrograph (Andor Model SR-750A). The spectrograph is equipped with three ruled gratings: 2400, 1200, and 300 grooves/mm, which are interchangeable under computer control and provide high and low resolution spectra in the wavelength range of 200–900 nm. An intensified gated CCD camera (Andor DH340T-18U-03) is coupled with the spectrograph output. The ICCD camera has 2048 × 512 pixels and is cooled to –15^{o}C by a Peltier cooler to reduce noise while working.

A laser energy of 25 mJ and detection duration of 1.5 μs are used with a gate width of 2 μs and a laser repetition rate of 4 Hz to improve repeatability and reduce the effects of continuous background created by bremsstrahlung. Twenty laser pulses are integrated to obtain each spectrum, and each experimental spectral intensity is the average of ten measurements in order to increase the stability and reduce the standard deviation of the spectral intensities.

Sample preparation. Six samples of the roots of *Angelica pubescens* (S48, S66, S168, S211, S285, S348) from Chongqing Academy of Chinese Medicine are analyzed in this work, and the concentrations of Ca, Mg, and K of the six samples, which are measured by the ICP-OES, are shown in Table 1. These six samples are gathered from different places of production and geographical environment, and they differ by the process of growth, which affect the concentrations of Ca, Mg, and K. Because the roots of *Angelica pubescens* are irregular and granular solid samples, the samples have to be preprocessed by tablet pressing in order to reduce the experimental errors and have a better ablation efficiency to get higher repeatability of the LIBS measurements [26]. Before the tablet pressing, all samples are dried in a drying oven at 60^{o}C for 8 h.

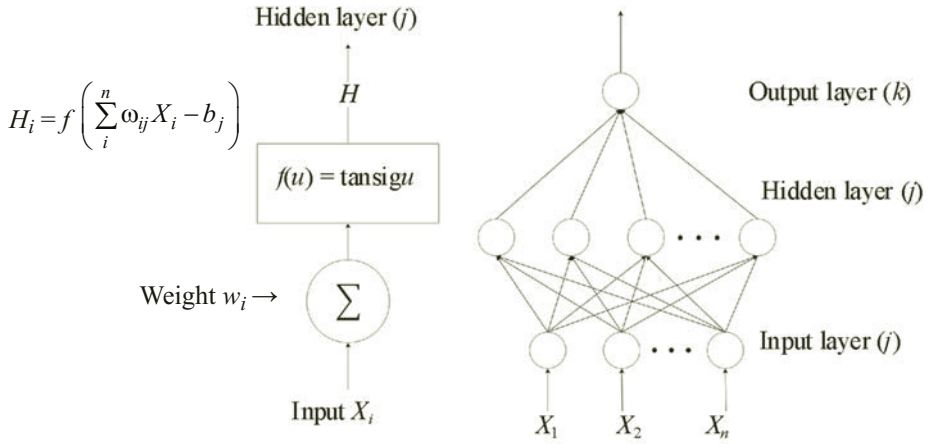

Fig. 2. Principle of an artificial neural network perceptron (a) and a three-layer neural network model (b).

TABLE 1. Concentrations (mg/kg) of Ca, Mg, and K of the Six Samples

Sample number	Ca	Mg	K
s46	4434	5967	17364
s66	6186	6084	32130
s168	18354	5160	31530
s211	14619	4584	93300
s285	19641	3584	82650
s348	12606	1968	26427

Then each sample is ground into powders and stirred uniformly for 2 h. These herbal powders are pressed to tablets (0.5 g, 13-mm diameter, and 2-mm thick) by a hydraulic press (2 min under a pressure of 10 tons for each tablet).

Artificial Neural Networks. The neural network algorithm is described in Fig. 2. An artificial neuron identifies a weighted sum of inputs X_i (i = 1, …, n) converging in the unit. Each input X_i is multiplied by a weight w_i, and the total input of the node is the weighted sum of the X_i. The number subtracts a threshold b and the perceptron applies a nonlinear transfer function (sigmoidal function) to get the output of the neuron [27]. The neurons are organized in layers to form a network. Common three-layer (input layer, hidden layer, and output layer) networks, also called a perceptron, have been used in the experiments, which is also presented in Fig. 2. Each neuron of the first (input) layer has a single input corresponding to the measured spectrum intensity at one wavelength. The outputs of the last (output) layer constitute the ANN results. Each neuron in this output layer is associated with one chemical element contributing to the spectrum. The number of neurons in the second layer (also called hidden layer) is a free parameter. All the neurons among three layers are related by the weighting factor w, threshold factor b, and the transfer function. The tansig function is chosen as the transfer function in this work.

Matlab software was used to build the artificial neural network model for quantitative analysis. In order to produce accurate results, the algorithm, which is also called a learning algorithm [28], needs to be trained (i.e., calibrated) with a set of reference spectra representative of the roots of *Angelica pubescens* targets. The training phase results in finding the best set of weights and bias values that would minimize the network output errors. This is done by using a back propagation algorithm, which is based on a gradient descent allowing the network — after a certain number of iterations — to find the best fit to the training set of input–output pairs. When the inputs (in our case, ten integrated spectral intensities and the average value for Ca, Mg, and K) are successively injected into the network, the weights change dynamically to reduce errors. This procedure is repeated until the network reaches a good result. The primary back-propagation parameters in this work are shown as following: learning rate 0.01, epochs 3000, max fail 10 and 1 hidden layer with 4 elements (neurons). Once the training phase is completed, a spectrum of unknown sample (i.e., intensities at selected wavelengths) is presented to the network, which quickly identifies (<ms) the corresponding elemental composition.

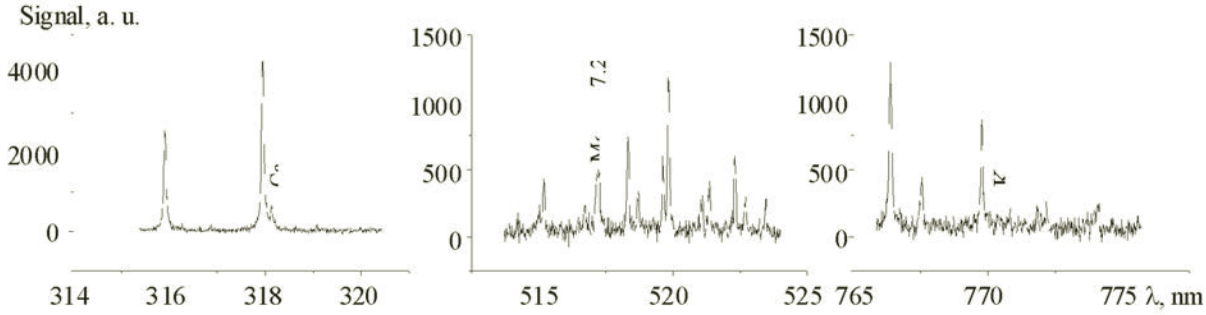

Fig. 3. Laser-induced spectra of Ca II 317.993 nm, Mg I 517.268 nm, and K I 769.896 nm.

TABLE 2. Predicted Concentrations (mg/kg) of Ca, Mg, and K in the Six Samples

Samples	External Standard Method			Artificial Neural Networks		
	Ca	Mg	K	Ca	Mg	K
s46	3134	6303	16,186	4851	5961	17,495
s66	7194	6213	37,055	7394	5923	31,737
s168	18,568	5025	38,661	17691	5201	32,471
s211	13,311	4304	93,165	14521	4510	102,321
s285	22389	3627	80,588	19124	3793	82,887
s348	10735	2038	21,889	11685	2042	22,544

Results and Discussion. Six samples of the roots of *Angelica pubescens* are quantitatively analyzed by the external standard method and the artificial neural network method. In order to compare the quantitative analysis performances of the two methods comprehensively, all six samples are used as both the training set and the prediction set to predict the concentrations of Ca, Mg, and K. The Ca II 317.993-nm, Mg I 517.268-nm, and K I 769.896-nm lines are chosen as the analysis spectral lines as shown in Fig. 3, because there are no obvious self-absorption and interferential spectral lines nearby.

In order to obtain the predicted concentrations of the two methods, all six samples are also used as predicted set to get predicted concentrations of Ca, Mg, and K. The predicted concentrations of the two methods are listed in Table 2.

To assess the quantitative performances between the two methods, six linear fittings of the predicted concentrations versus the standard concentrations are established as shown in Fig. 4.

Five parameters are calculated to verify the accuracy and the stability of the predicted concentrations of Ca, Mg, and K by the two methods. They are the linear correlation coefficients (R^2) of linear fitting of the predicted concentrations versus the standard concentrations and the average relative errors (AREs), the maximum relative errors (MREs), the average relative standard deviations (ARSDs), and the maximum relative standard deviations (MRSDs) of the predicted concentrations among the six samples. R^2 represents the accuracy of the quantitative analysis, and ARE, MRE, ARSD, and MRSD represent the stability of the quantitative analysis. The relative error and relative standard deviation can be calculated from the following formula:

$$\mathrm{RE} = |(\bar{x} - \mu)/\mu| \times 100\% ,$$

where $\bar{x}$ is the average value of the predicted concentrations, and μ is the standard concentration;

$$RSD = \frac{1}{\bar{x}} SD = \left(\frac{1}{\bar{x}} \sqrt{\frac{\sum_{i=1}^{n} (xi - \bar{x})^2}{n-1}} \right),$$

where x_i is a value of the predicted concentration, and n is the predicted times.

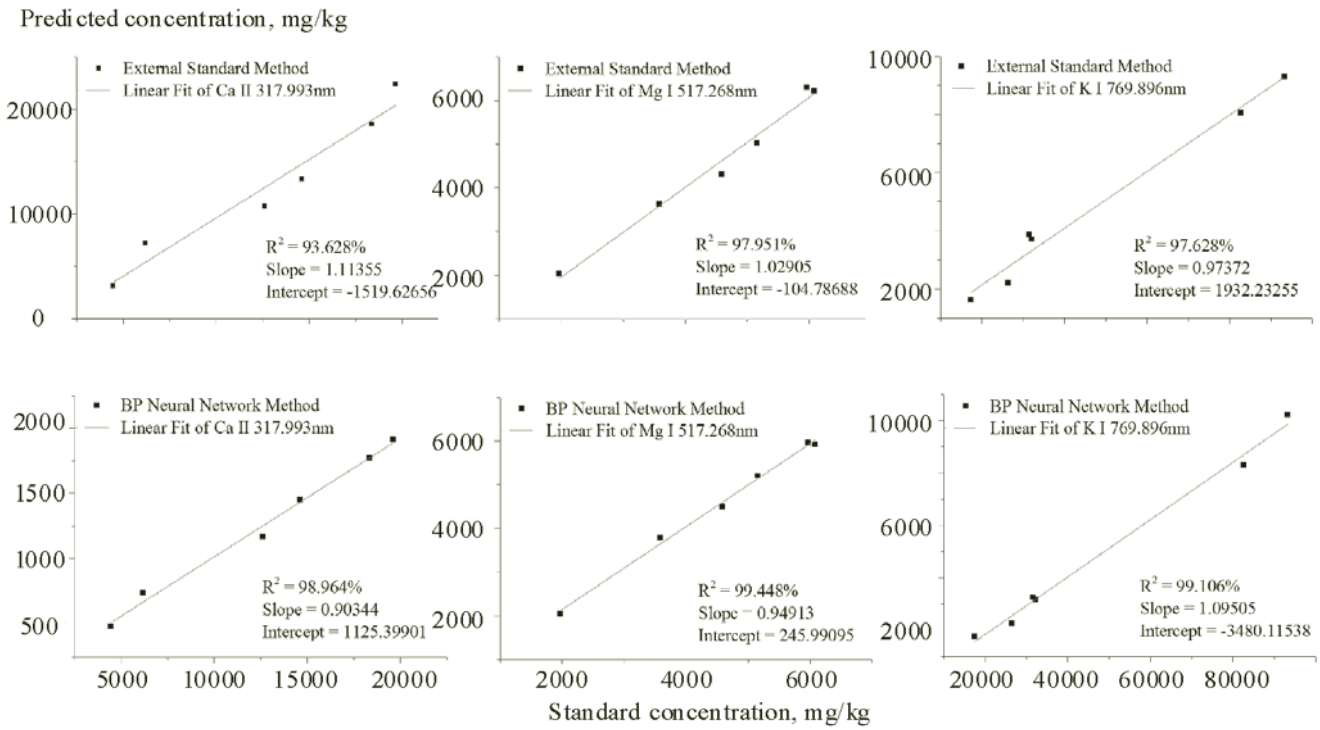

Fig. 4. Linear fittings of the predicted concentrations versus the standard concentrations of Ca, Mg, and K by the external standard method and the artificial neural network method.

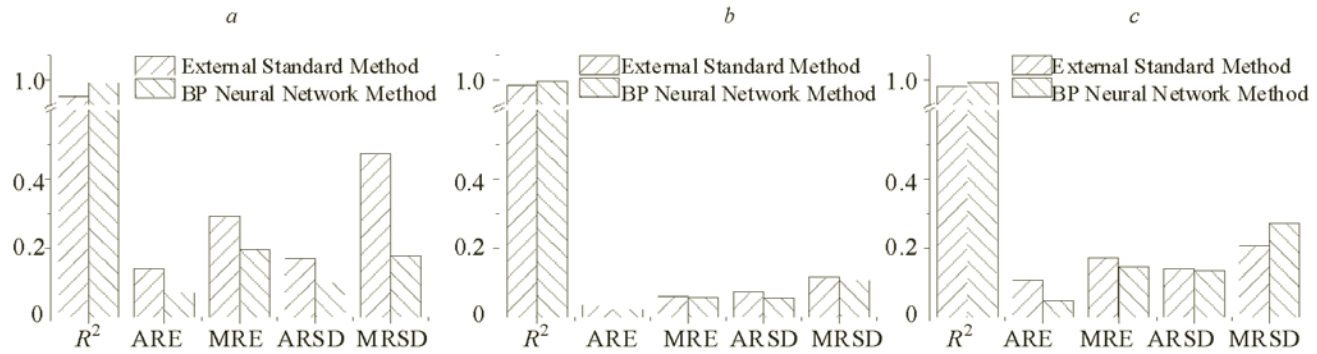

Fig. 5. Quantitative performances of the external standard and artificial neural network methods in the analysis of Ca (a), Mg (b), and K (c).

TABLE 3. Quantitative Performances of Ca, Mg, and K by the Two Methods

Evaluation parameters	External Standard Method			Artificial Neural Networks		
	Ca	Mg	K	Ca	Mg	K
R^2	0.9363	0.9795	0.9763	0.9896	0.9945	0.9911
ARE	14.09%	3.54%	10.76%	7.19%	2.46%	4.94%
MRE	29.30%	6.09%	17.17%	19.53%	5.85%	14.69%
ARSD	17.00%	7.35%	14.00%	10.13%	5.68%	13.49%
MRSD	47.38%	11.62%	20.73%	17.78%	10.71%	27.14%

The five evaluation parameters (R^2, AREs, MREs, ARSDs, and MRSDs) of the quantitative analysis by the two methods are listed in Table 3 and Fig. 4.

For the prediction accuracy, it can be observed in Fig. 5 that the linear correlation coefficients (R^2) of the artificial neural network method are 0.9896, 0.9945, and 0.9911 for Ca, Mg, and K, respectively, while the R^2 of the external standard method are 0.9363, 0.9795, and 0.9763, respectively. Therefore in this work, the artificial neural network method provides a more accurate quantitative analysis than the external standard method.

For the prediction stability, in Fig. 5, it can be observed that the average and maximum relative errors (AREs and MREs) of the artificial neural network method are 7.19, 2.46, 4.94, and 19.53, 5.85, 14.69 % for Ca, Mg, and K, respectively, while the AREs and MREs of the external standard method are 14.09, 3.54, 10.76, and 29.30, 6.09, 17.17 %, respectively. The average and maximum relative standard deviations (ARSDs and MRSDs) of the predicted concentrations obtained by the artificial neural network method for Ca, Mg, and K are 10.13, 5.68, 13.49, and 17.78, 10.71, 27.14 %, respectively. The ARSDs and MRSDs of the concentrations predicted by the external standard method are 17.00, 7.35, 14.00, and 47.38, 11.62, 20.73 %, respectively. The results above show that all the AREs, MREs, ARSDs, and MRSDs of Ca and Mg by the artificial neural network method are better than those by the external standard method. Meanwhile, ARE, MRE and ARSD of K by the artificial neural network method are also better than by the external standard method except MRSD. So we can also conclude that the artificial neural network method gives more stable quantitative analysis performance than the external standard method in this work.

Overall, the artificial neural network method gives better quantitative performance than the external standard method, because artificial neural network can use more information besides peak heights, if such information is considered important to the predicted concentrations of elements. But the deficiency of artificial neural network is exposed by its MRSD of K in this work. For the artificial neural network method, theoretically, more input neurons will bring better network training and prediction stability. ANN training is inadequate in this work. Since only 11 input neurons are used, which reduces the prediction stability.

Conclusions. The aim of this work is to evaluate the potential of quantitative analysis of beneficial elements in traditional Chinese medicine such as the root of *Angelica pubescence* by the LIBS technology combined with the artificial neural network method. The LIBS spectra of six *Angelica pubescence* root samples are collected. What is more, the concentrations of Ca, Mg, and K in the six samples are determined by the external standard method and the artificial neural network method. All the six samples are used as both the training set (for calibration) and the prediction set (for prediction). Calibration models are established, and the predicted concentrations of all six samples are determined by two methods. The obtained results clearly show that the LIBS technique combined with the artificial neural network method gives more accurate and stable quantitative analysis performance while detecting the elements of Ca, Mg, and K in *Angelica pubescence* root samples than the external standard method. It is proved that the artificial neural network method is a favorable method for analyzing traditional Chinese medicine quantitatively.

Acknowledgments. This work is finically supported by Science Research Funds of Chongqing Municipal Education Commission (KJ1500436), Key Project of Foundation and Advanced Technology Research Project of Chongqing (cstc2015jcyjB0358), Scientific Research Foundation for the Returning Overseas Chinese Scholars, State Education Ministry, and Foundation and Advanced Technology Research Project of Chongqing (cstc2016jcyjA2293).

REFERENCES

1. T. Fujioka, K. H. Furumi, and H. Okabe, *Chem. Pharm. Bull.*, **47**, 96–100 (1999).
2. M. Senila, A. Drolc, and A. Pintar, *J. Anal. Sci. Technol.*, **5**, 1–9 (2014).
3. X. D. Yuan, K. H. Ling, and C. W. Keung, *Phytochem. Anal.*, **20**, 293–297 (2009).
4. S. Arpadjan, G. Çelik, and S. Taşkesen, *Food Chem. Toxicol*., **46**, 2871–2875 (2008).
5. P. C. Zheng, H. D. Liu, and J. M. Wang, *Anal. Methods*, **6**, 2163–2169 (2014).
6. S. Kashiwakura and K. Wagatsuma, *Anal. Sci.*, **29**, 1159–1164 (2013).
7. B. Chen, H. Kano, and M. Kuzuya. *Anal. Sci.*, **24**, 289–291 (2008).
8. M. Y. Yao, L. Huang, and J. Zheng, *Opt. Laser Technol.*, **52**, 70–74 (2013).
9. L. Huang, M. Y. Yao, and J. L. Lin, *J. Appl. Spectrosc*., **80**, 957–961 (2014).
10. P. C. Zheng, H. D. Liu, and J. M. Wang, *J. Anal. At. Spectrom.*, **30**, 867–874 (2015).
11. Y. Li, Y. Lu, and R. E. Zheng, *Spectrosc. & Spectr. Anal.*, **32**, 582–585 (2012).
12. M. Yao, J. Lin, and M. Liu, *Appl. Opt.*, **51**, 1552–1557 (2012).

13. L. Huang, M. Yao, Y. Xu, and M. Liu, *Appl. Phys. B*, **111**, 45–51 (2013).
14. D. Zhu, J. Chen, and J. Lu, *Anal. Methods*, **4**, 819–823 (2012).
15. Y. Cai, P. C. Chu, and S. K. Ho, *Front. Phys.*, **7**, 670–678 (2012).
16. Y. Wang, W. L. Liu, and Y. F. Song, *Chem. Phys.*, **447**, 30–35 (2015).
17. E. Jobiliong, H. Suyanto, and A. M. Marpaung, *J. Appl. Spectrosc.*, **69**, 115–123 (2015).
18. Y. Zhang, G. Xiong, and S. Li, *Combust. Flame*, **160**, 725–733 (2013).
19. Y. Yuan, S. Li, and Q. Yao, *Proc. Combust. Inst.*, **35**, 2339–2346 (2015).
20. Y. Zhang, S. Li, Y. Ren, and Q. Yao, *Proc. Combust. Inst.*, **35**, 3681–3688 (2015).
21. E. C. Ferreira, D. M. Milori, and E. J. Ferreira, *Spectrochim. Acta*, *B*, **63**, 1216–1220 (2008).
22. P. Inakollu, T. Philip, and A. K. Rai, *Spectrochim. Acta*, *B*, **64**, 99–104 (2009).
23. L. X. Sun, H. B. Yu, and Z. B. Cong, *Acta Opt. Sin.*, **30**, 2757–2765 (2010).
24. V. Motto-Ros, A. S. Koujelev, and G. R. Osinski, *J. Europ. Opt. Soc. Rapid Publ.*, **3**, 08011 (2008).
25. S. Y. Oh, F. Y. Yueh, and J. P. Singh, *Appl. Opt.*, **49**, C36–C41 (2010).
26. P. C. Zheng, M. J. Shi, and J. M. Wang, *Plasma Sci. Technol*, **17**, 664–670 (2015).
27. J. B. Sirven, B. Bousquet, and L. Canioni, *Anal. Bioanal.Chem.*, **385**, 256–262 (2006).
28. R. Beale and T. Jackson, *Neural Computing – An Introduction*, CRC Press, Florida, USA (1990).